Mechanism of co-operation of mutant *IL-7Rα* and mutant *NRAS* in acute lymphoblastic leukemia: role of MYC

Hila Winer,[1*] Wenqing Li,[1*] Gisele Rodrigues,[1] Tim Gower,[1] Thomas Joshua Meyer,[2] Julie Hixon[1] and Scott K. Durum[1]

[1]Cytokines and Immunity Section, Cancer Innovation Laboratory (CIL) and [2]CCR Collaborative Bioinformatics Resource (CCBR), National Cancer Institute (NCI), National Institutes of Health (NIH), Frederick, MD, USA

**HW and WL contributed equally as first authors.*

Correspondence: S. Durum
durums@mail.nih.gov

Received: May 25, 2023.
Accepted: November 22, 2023.
Early view: November 30, 2023.

https://doi.org/10.3324/haematol.2023.283559

Supplementary Methods

Flow cytometry

Cell suspensions were blocked by CD16/32 Fc receptor block (Biolegend) then stained with: anti-Thy1.2 APC-Cy7 (Biolegend), anti-CD4 Alexa 405 (Caltag), anti-CD8 APC (Biolegend), anti-TCRβ Alexa Fluor 700 (Biolegend), anti-TCRγ/δ PE-Cy7 (Biolegend) and anti-TCRVa2 PE (Pharmingen). Flow cytometric analysis was performed on an LSRIISORP (BD). Data analysis was performed using FlowJo (Tree Star, Inc.).

Immunoblotting analysis

Proteins were separated by 4-12% NUPAGE gel electrophoresis and transferred to a polyvinylidene difluoride membrane. The membrane was blocked with (5% (w/v) milk in TBS buffer with 0.1% Tween-20 (TBST), for 1 h at room temperature (RT), incubated with primary antibody (overnight, 4 °C), washed in TBST ×3, incubated with secondary antibody (1h, RT), and washed (as above). Finally, the membrane was treated with an enhanced chemiluminescence reagent (ECL- Thermo- Fisher Scientific) and observed under chemiluminescence Amersham Imager 680 (GE healthcare life science). Primary antibodies used: c-Myc, BAK-1, p-AKT/AKT, p-GSKα/β, GSKα/β, p-cMyc (S62), p-cMyc (T58), p-ERK, ERK, PLK-1, PIM-1 and p-BAD/BAD were from Cell Signaling. Other primary antibodies were against BCL-2 (Santa Cruz), NRAS (Abcam), humanIL7R (R&D systems), GAPDH (Novus) and Actin (Sigma). Secondary antibodies used: anti-Rabbit-HRP, anti-Mouse-HRP from Cell Signaling and anti-goat-HRP from Invitrogen.

shRNA analysis

Primary thymocytes and mouse thymic D1 cell line were transduced with mutIL7Rα-T2A-mutNRAS in pMIG vector with GFP expression. D1 cells were sorted for GFP positive cells and transduced with shRNA using retroviral vector IRES-mCherry containing shRNA under human U6 promoter: *shScrambled*, *shMyc-1891* and *shMyc-2105* (all expressed with *mCherry)* [1]. Cells were monitored by flow-cytometry for GFP and mCherry for 10 days.

Quantitative Real time PCR analysis (qRT-PCR)

mRNA was isolated using RNeasy mini kit (Qiagen) and reverse transcribed to cDNA using high-capacity cDNA reverse transcription kit (applied biosystems). Quantitative RT-PCR (qRT-PCR) was performed on isolated cDNA using TaqMan probe-based chemistry, using LightCycler 480 master kit (Roche). All probe sets were from Applied Biosystems, Life Technologies (Thermo Fisher scientific). Each experiment was done in triplicate and compared to NRT.

Immunohistochemistry staining

Formalin fixed mouse spleens were stained for immunohistochemistry (IHC) against c-Myc (1:40, Abcam ab32072, HIER Citrate). Breast and colon carcinoma, and D1 cells overexpressing c-Myc were used and positive controls. Non-specific Ab and isotype control were used as negative controls. Whole Slide Imaging (WSI) was performed with an Aperio ScanScope XT (Leica) at 200X in a single z-plane. Analysis was performed using HALO (Indica Labs) and included AI nuclear detection and positivity thresholding to quantify positive cells based on positive controls and assessed by a veterinary pathologist. Staining intensity was scored using a scale of 0 – 3 and tumor H-score [2] was calculated [1 × (% cells 1+) + 2 × (% cells 2+) + 3 × (% cells 3+)].

RNA sequencing, DEG and GSEA analysis

mRNA samples were pooled and sequenced on HiSeq4000 using Illumina TruSeq Stranded mRNA Library Prep and paired-end sequencing. Reads were trimmed for adapters and low-quality bases using Cutadapt (v1.18;) before alignment with the reference genome (Mouse - mm9) and the annotated transcripts using STAR v2.5 [3, 4]. Then, RSEM v1.3.0 was used to quantify expression [5]. Downstream analysis and visualization were performed within the NIH Integrated Analysis Platform (NIDAP) using R programs developed on the Foundry platform (Palantir Technologies). Genes were filtered for low counts (<1 cpm), and quantile normalized prior to differential expression using limma-voom v3.38.3 [6]. Gene set enrichment analysis (GSEA) was performed using fGSEA v1.8.0 [7]. Differentially expressed genes ($p<0.01$, FC>2) were further analyzed and pathways with an adjusted $p<0.01$ were considered significant in the enrichment analysis. Code is available in GitHub: https://github.com/NIDAP-Community/Cooperation-of-mutant-IL7R-and-NRAS-in-ALL.

Mass Spectrometry analysis

Cell lysates from duplicate samples were digested with trypsin using the filter-aided sample preparation (FASP) protocol as previously described [8]. Resultant peptides were desalted by C18 SepPak cartridge (Waters) and fractionated by high pH reversed-phase spin columns (Thermo). Each fraction of each sample was separated on a 75 µm x 15 cm, 2 µm Acclaim PepMap reverse phase column (Thermo) using an UltiMate 3000 RSLCnano HPLC (Thermo) at a flow rate of 300 nL/min followed by online analysis by tandem mass spectrometry using a Thermo Orbitrap Fusion mass spectrometer. Parent full-scan mass spectra were collected in the Orbitrap mass analyzer set to acquire data at 120,000 FWHM resolution; ions were fragmented at HCD normalized energy 35%, stepped ± 3%, and the product ions analyzed in the ion trap. Proteome Discoverer 2.2 (Thermo) was used to search the data against murine proteins from the UniProt database using SequestHT. The Percolator node was used to score and rank peptide matches using a 1% false discovery rate. Label-free quantitation of peptides was performed from extracted ion chromatograms using the Precursor Ions Quantifier node.

References

1. Zuber, J., et al., *An integrated approach to dissecting oncogene addiction implicates a Myb-coordinated self-renewal program as essential for leukemia maintenance.* Genes Dev, 2011. **25**(15): p. 1628-40.
2. McCarty, K.S., Jr., et al., *Estrogen receptor analyses. Correlation of biochemical and immunohistochemical methods using monoclonal antireceptor antibodies.* Arch Pathol Lab Med, 1985. **109**(8): p. 716-21.
3. Dobin, A., et al., *STAR: ultrafast universal RNA-seq aligner.* Bioinformatics, 2013. **29**(1): p. 15-21.
4. Martin, M., *Cutadapt removes adapter sequences from high-throughput sequencing reads.* EMBnet J. , 2011. **17, 3. 10.14806/ej.17.1.200**.
5. Li, B. and C.N. Dewey, *RSEM: accurate transcript quantification from RNA-Seq data with or without a reference genome.* BMC Bioinformatics, 2011. **12**: p. 323.
6. Ritchie, M.E., et al., *limma powers differential expression analyses for RNA-sequencing and microarray studies.* Nucleic Acids Res, 2015. **43**(7): p. e47.
7. Liberzon, A., et al., *Molecular signatures database (MSigDB) 3.0.* Bioinformatics, 2011. **27**(12): p. 1739-40.
8. Wisniewski, J.R., et al., *Universal sample preparation method for proteome analysis.* Nat Methods, 2009. **6**(5): p. 359-62.

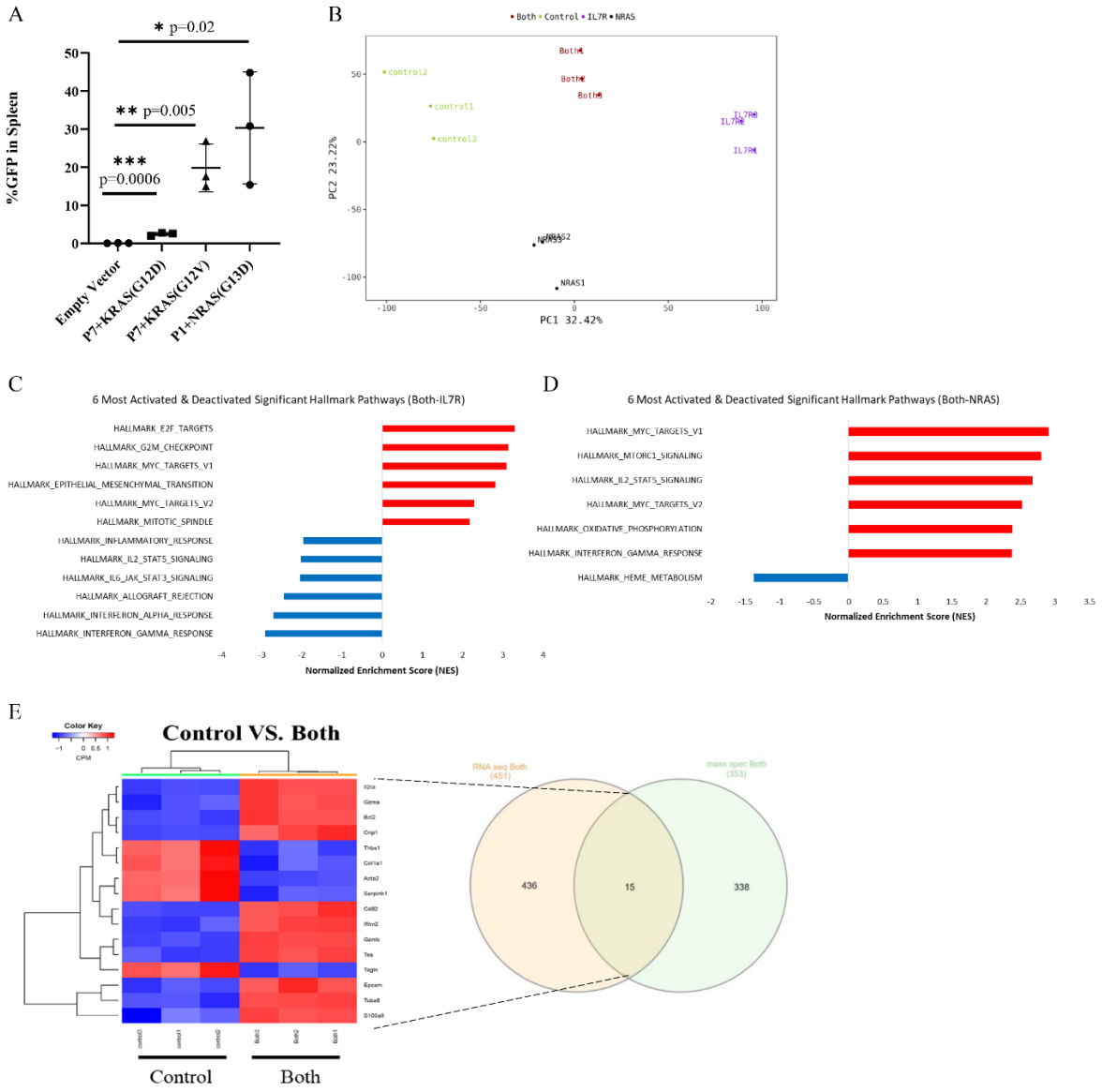

Figure S1. Identifying the molecular pathway that leads to ALL caused by mutIL7R and mutNRAS. (A) Double negative primary thymocytes were transduced and injected to RAG-/- mice with the following combinations: mutIL7R(P7) + KRAS(G12D or G12V) or mutIL7R(P1) + NRAS(G13D). Spleen was collected after disease appearance and analyzed by flow cytometric for positive GFP leukemic cells. (B) PCA (principal component analysis) plot of the 12 samples colored by treatment group: empty vector (Control), mutIL7R (IL7R), mutNRAS (NRAS) and both mutations combined (Both). (C-D) Bar charts showing GSEA (gene set enrichment analysis) normalized enrichment scores from the 6 most activated (red bars) and 6 most deactivated (blue bars) Hallmark collection pathways: (C) enriched pathways from a comparison contrast of the group with both mutations combined (Both) relative to that with mutIL7R alone, (D) enriched pathways from a comparison contrast of the group with both mutations combined (Both) relative to mutNRAS alone. (E) Genes and proteins that were up or down regulated in both RNA sequencing and mass spectrometry were analyzed by Venn Diagram and presented with heat map. Significantly differential genes from the Both vs. Control contrast of our RNA-seq (yellow circle) and mass spectrometry (green circle) analyses were intersected using a Venn Diagram. Those differential genes identified in both analyses are presented in the expression heatmap. Heat is row-centered and normalized expression z-scores, colored annotation bars at the top show treatment groups, and phylograms on the top and side are the result of unsupervised clustering of samples and genes, respectively.

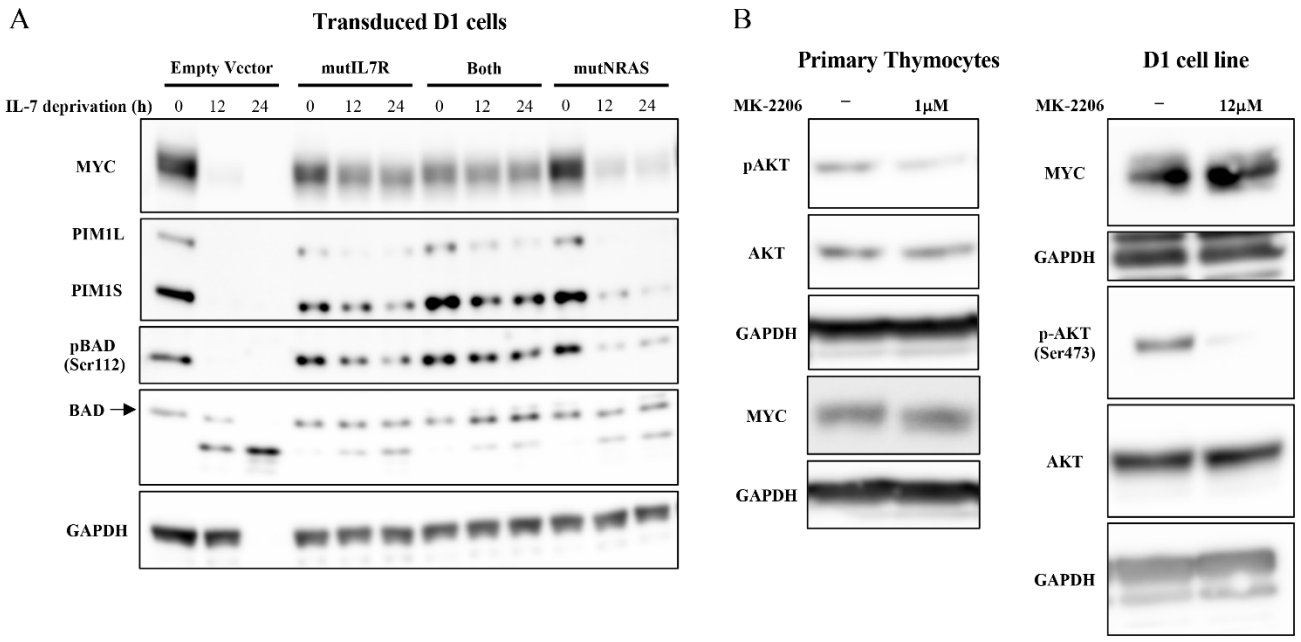

Figure S2. Changes in pre/anti oncogenic related protein in D1 thymic cell line expressed and MYC transitional inhibition on the background of mutIL7R and mutNRAS.
(A) D1 cells were transduced with: Empty vector, mutIL7R, mutNRAS or combination of both mutations (Both) and sorted for GFP. The sorted cells were cultured in the presence of IL7 (time point 0) or deprivation of IL7 in different time point. Cells were lysed and analyzed by western blot. (B) Primary thymocytes and D1 cell were transduced with mutIL7R and mutNRAS. 72h after transduction cells were treated with MK-2206 1mM for 24h, lysed and analyzed by western blot.

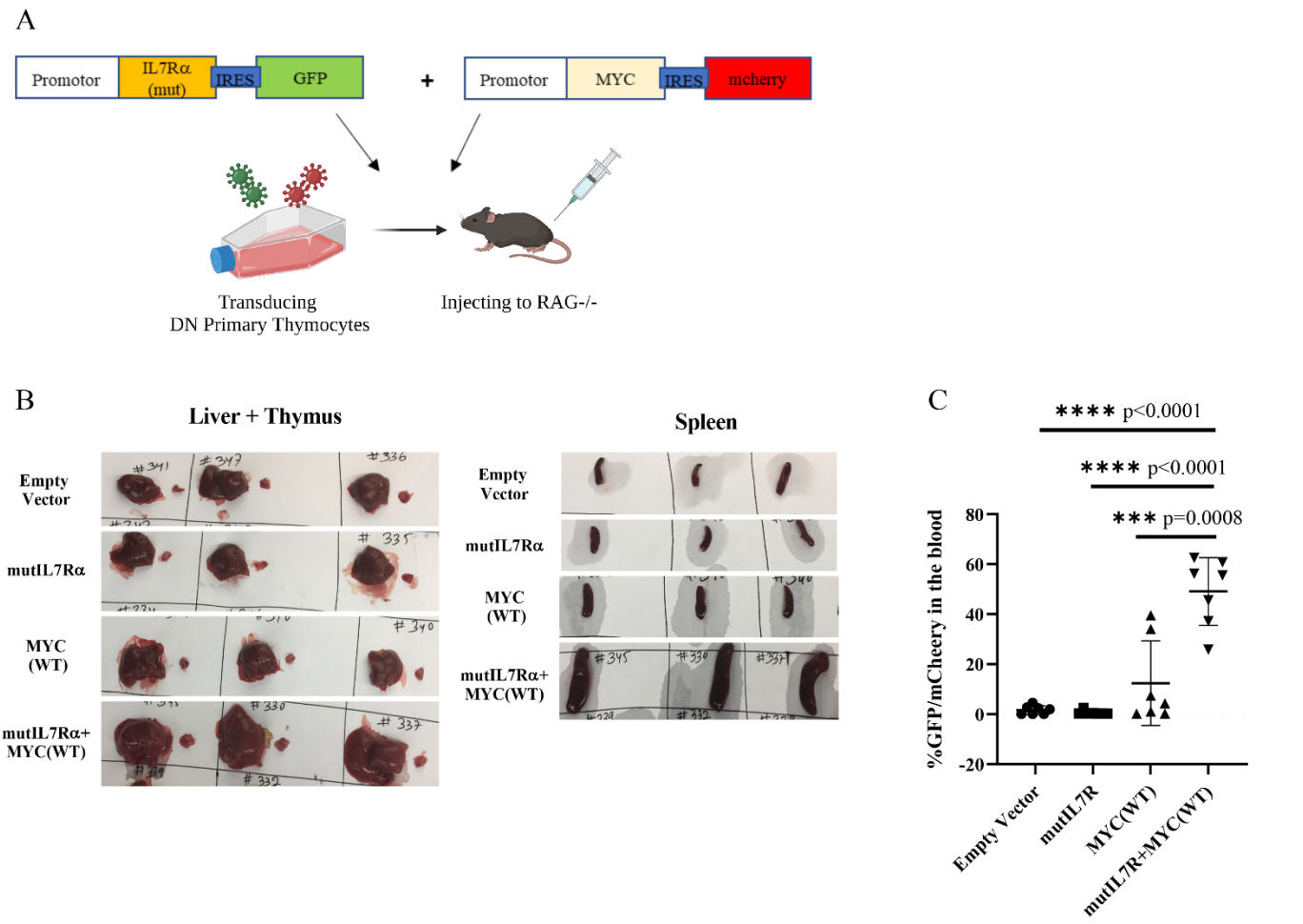

Figure S3. **Leukemia formation in RAG-1-/- mice injected with thymocytes containing mutIL7R and MYC overexpression.**

(A) Schematic presentation of the mutIL7R and MYC expression in thymocytes injected to RAG1-/- mice. (B) Representative images of liver, thymus and spleen taken from the different mice groups. (C) Quantification of flow cytometric analysis of GFP and mCherry double positive expression in the different groups from blood.

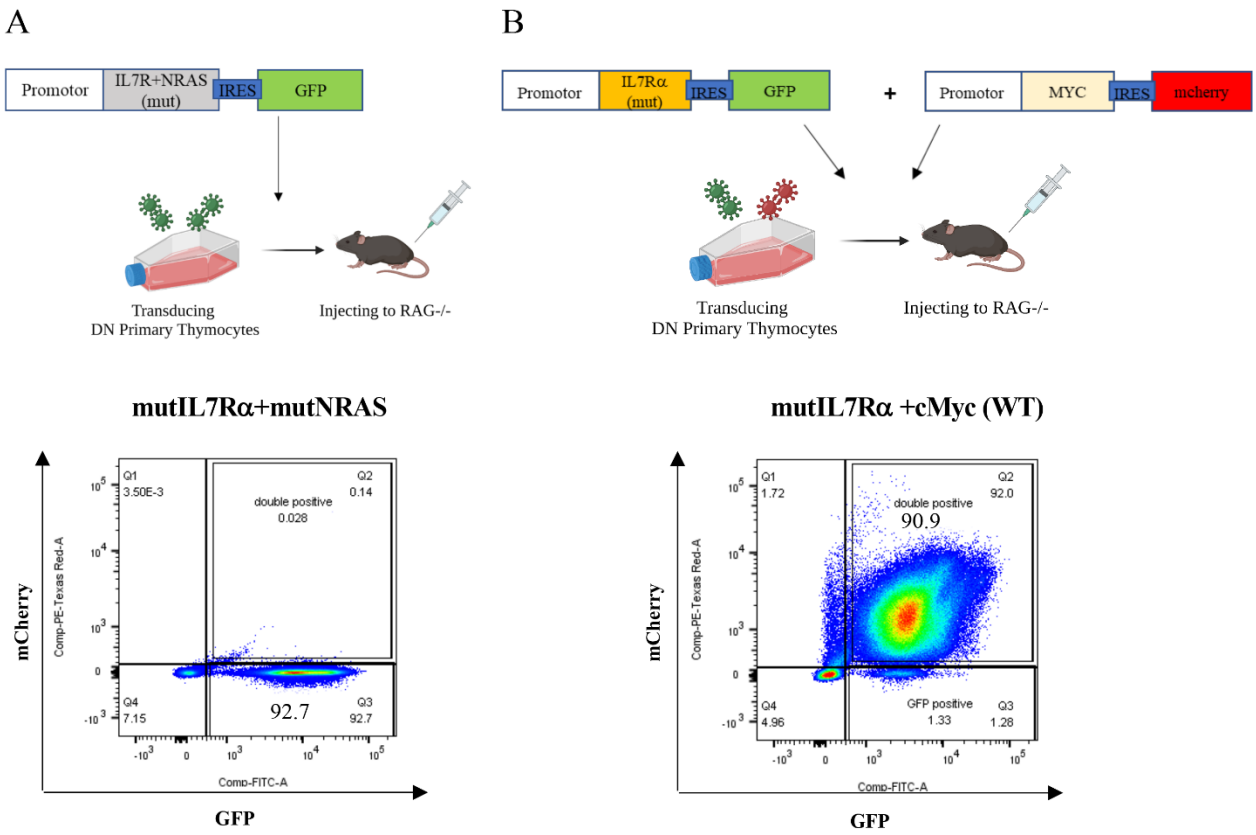

Figure S4. Experiment design presentation of the two ALL model using mutIL7R with either mutNRAS or MYC.

(A) Schematic presentation of mutIL7R and mutNRAS expressed with GFP and the flow cytometry presentation gating on GFP leukemic cells. (B) Schematic presentation of mutIL7R expressed with GFP together with MYC expressed with mCherry and the flow cytometry presentation gating on GFP and mCherry double positive leukemic cells.

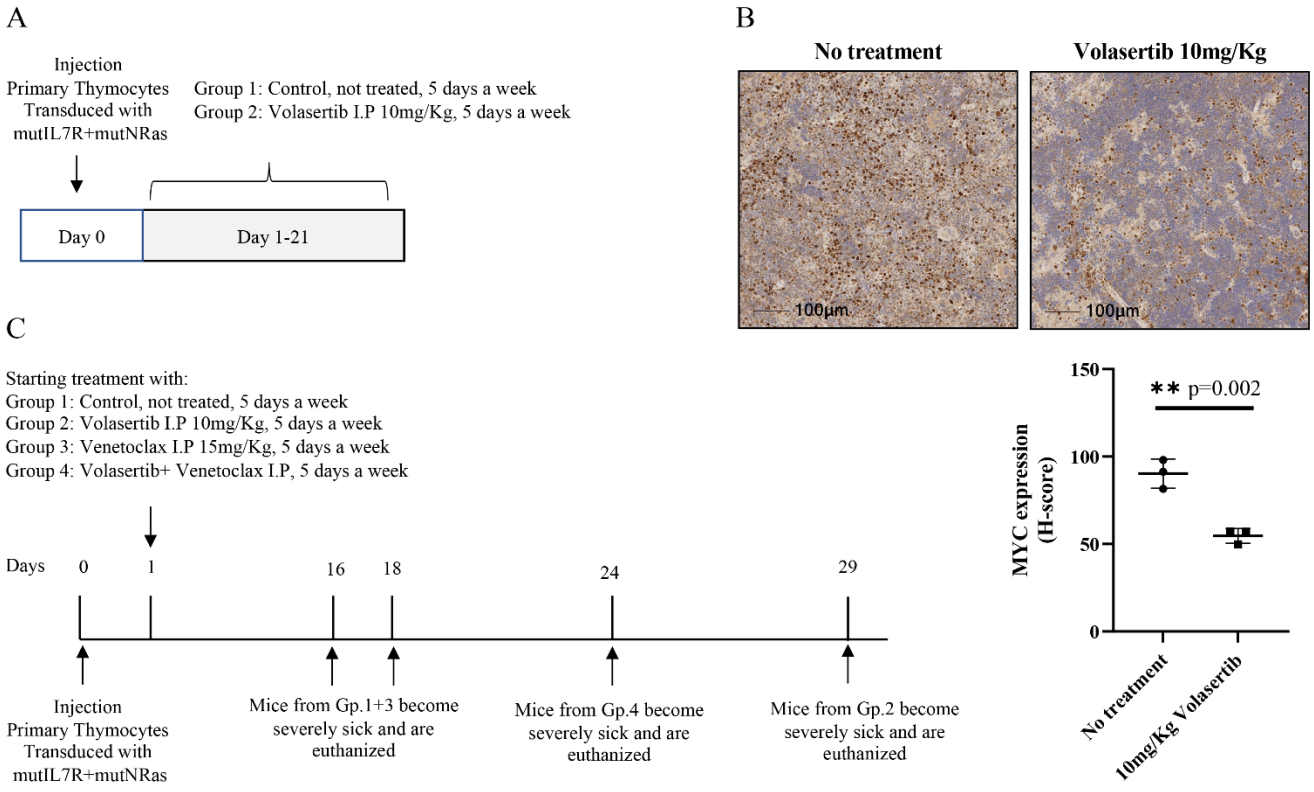

Figure S5. Delaying ALL progression caused by mutIL7Rα and mutNRAS using PLK-1 inhibitor, Volasertib

(A) Schematic presentation of Volasertib treatment in RAG1-/- mice. (B) Top: representative image of immunohistochemistry staining of spleen tissue against MYC, no treatment (N=3) and Volasertib 10mg/Kg treated (N=3); Bottom: H-score compared between with or without treatment. (C) Schematic presentation of the chronological events during treatment with Volasertib and Venetoclax.

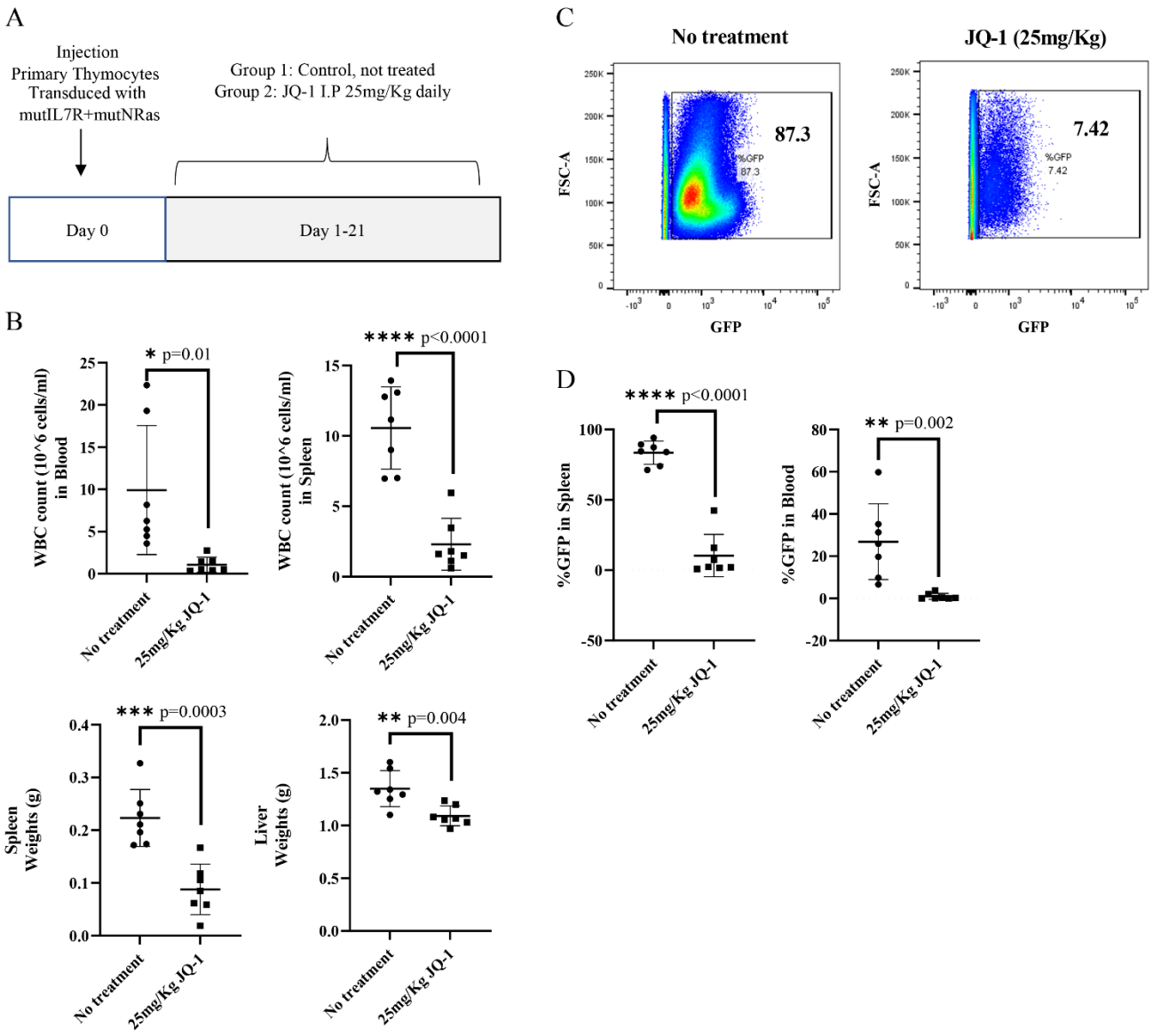

Figure S6. Delaying ALL progression caused by mutIL7Rα and mutNRAS using BET bromodomain inhibitor, JQ-1.

RAG1-/- mice injected with thymocytes transduced with mutIL7R and mutNRAS thymocytes, were treated with JQ-1 for 21 days (A) Schematic presentation of JQ-1 treatment in RAG1-/- recipient mice. (B) Comparing control-no treatment mice (N=7) with mice treated with JQ-1 25mg/Kg (N=7). Upper panel: WBC count in the spleen and blood. Lower panel: spleen and liver weights. (C) Percentage of GFP expression in splenocytes with or without JQ-1 treatment. (D) Quantification of the GFP percentage in the spleen and peripheral blood from each group (N=7).

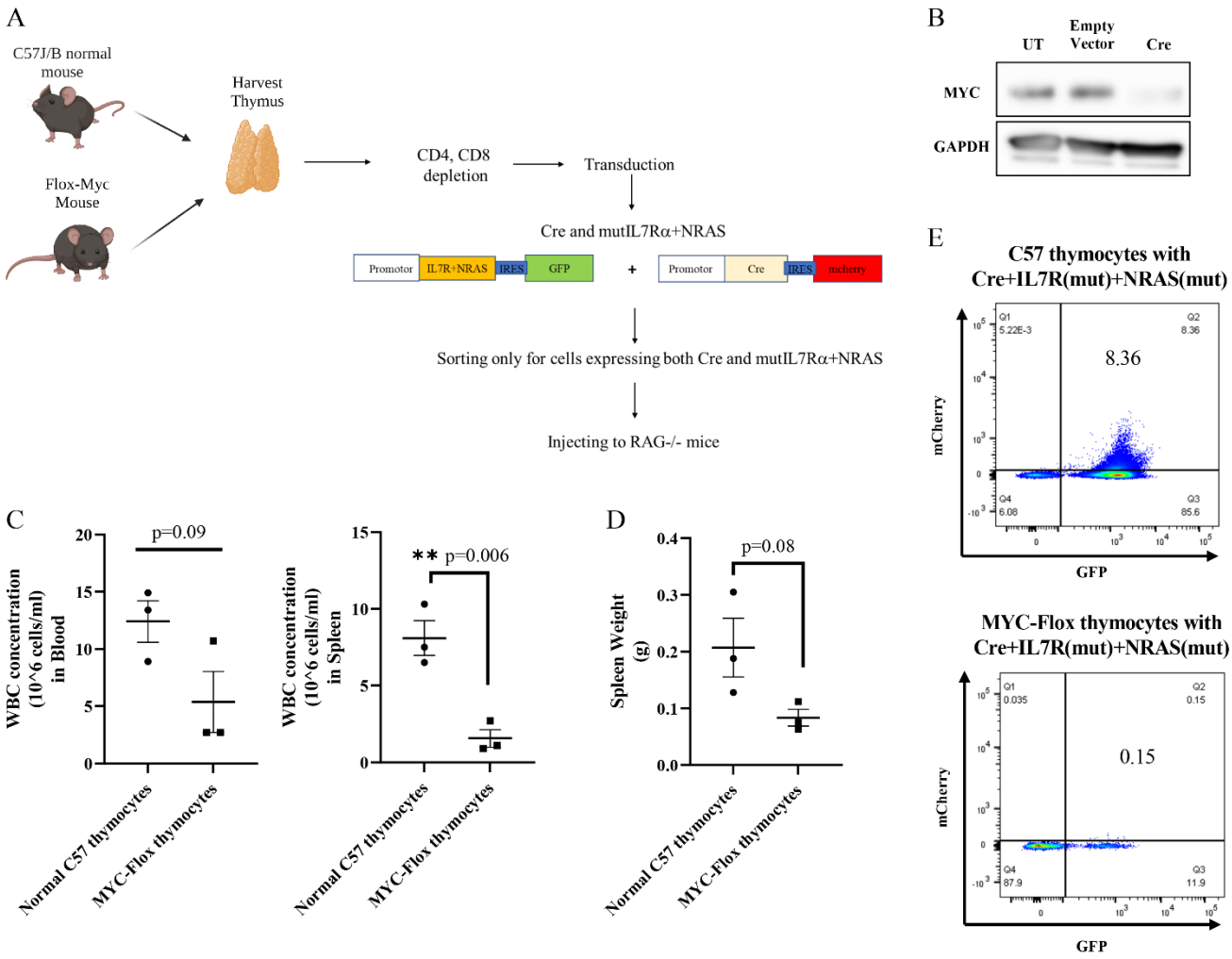

Figure S7. MYC knockdown delay the progress of ALL in mice

(A) Schematic presentation of thymocytes isolation from either Flox Myc mice (N=3) or Normal C57 (N=3), transduced with Cre (together with mCherry) and mutIL7R and NRAS (together with GFP), followed by sorting for double positive cells before injecting into RAG1-/- mice. (B) Western blot analysis of MYC protein from primary thymocytes isolated from Flox myc mice either un-transduced (UT) or transduced with empty vector or Cre. 21-35 days after injection mice were euthanized and analyzed for (C) WBC concentration (D) Spleen weights (E) Flow cytometry analysis comparing both groups, higher percentage of double positive fluorophore (GFP and mCherry) indicates for T-ALL development.

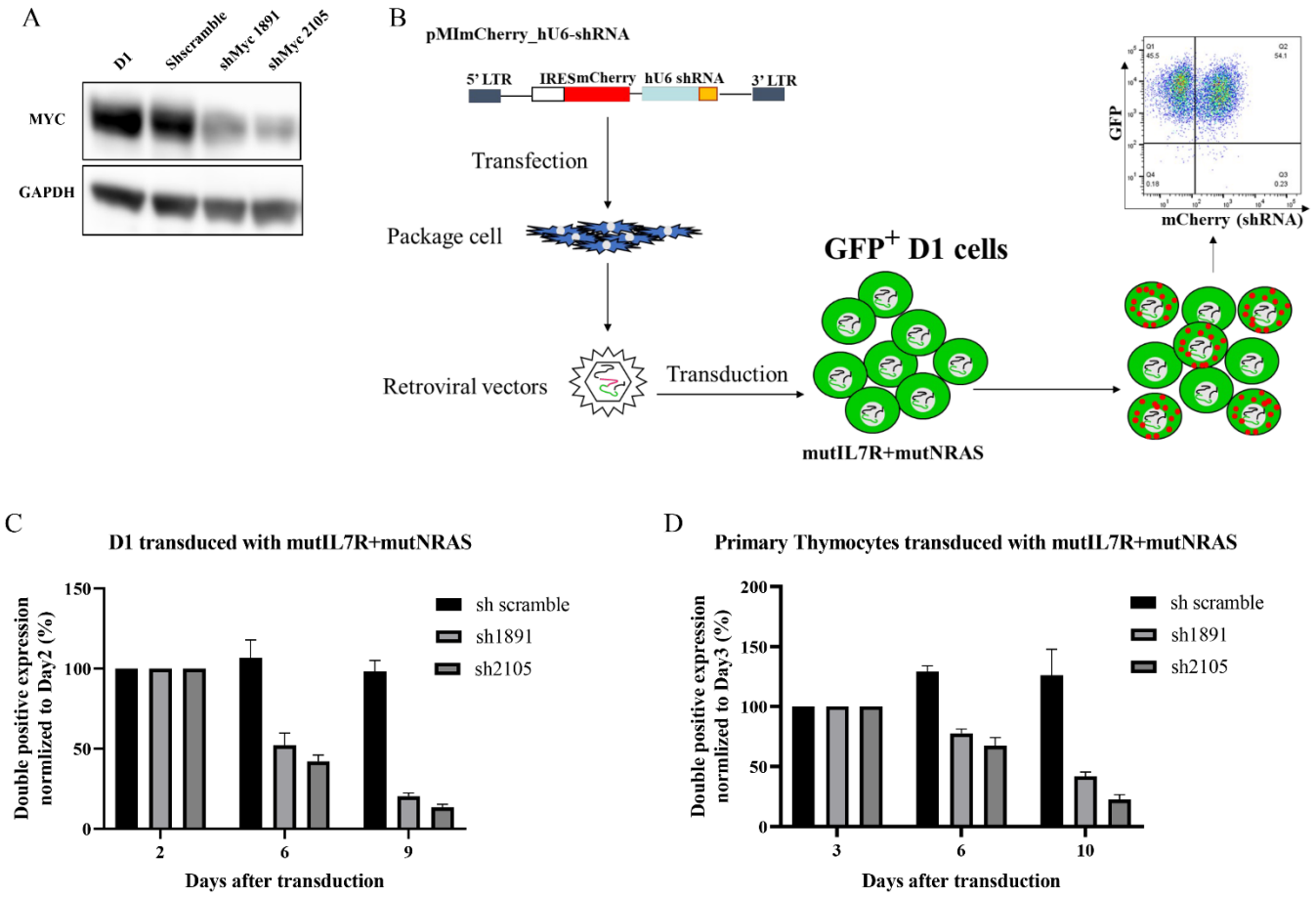

Figure S8. MYC knockdown decreases cell proliferation in thymic cell line.
(A) D1 cell line transduced with sh-scramble or Myc shRNA: 1891 or 2105 sequence, 72h after transduction cells were lysed and analyzed by western blot. (B) Schematic presentation of D1 cells transduction with both mutIL7R and mutNRAS (together with GFP) and shRNA (together with mCherry) analyzed by flow cytometry. (C+D) D1 cell line or thymocytes were transduced with mutIL7R+mutNRAS and shRNA and monitored over time by flow cytometry for GFP and mCherry signal (percentage of double positive cells); (C) D1 cell line, (D) Primary thymocytes taken from C57BL/6J thymus.

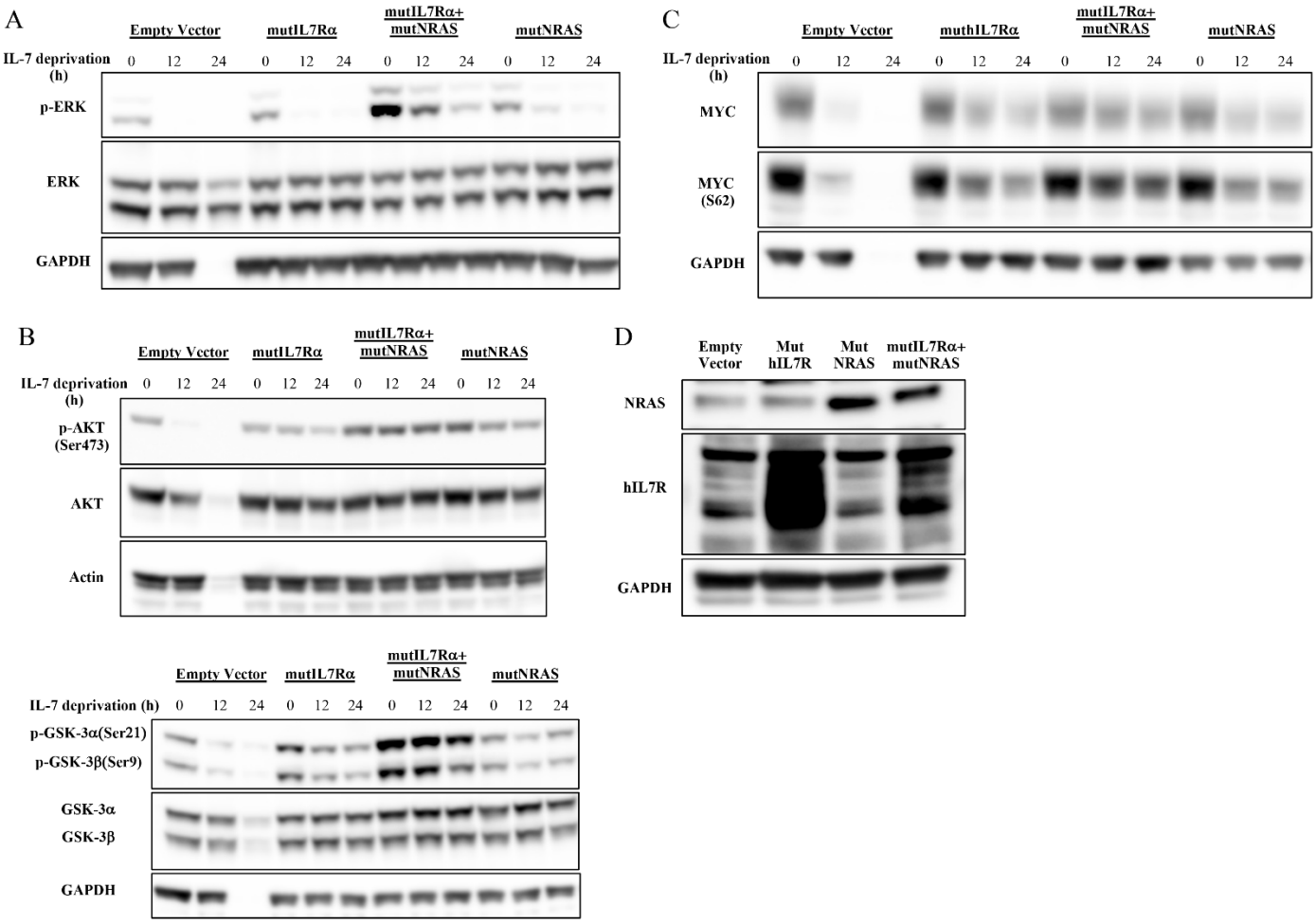

Figure S9. Involvement of the PI3K/AKT and MEK/ERK pathways on regulating MYC in thymic cell line
D1 cell line were transduced with either: empty vector, mutant IL7R, mutant NRAS or both IL7R and NRAS and sorted for GFP. The sorted cells were either treated with IL-7 (time point 0) or deprived from IL-7 treatment for 12h and 24h time points then cells were lysed and analyzed by western blot for: (A) p-ERK and ERK. (B) p-AKT, AKT, p-GSK-3α/β and GSK-3α/β. (C) MYC and p-Myc (Ser 62). (D) Primary thymocytes transduced with empty vector, muthIL7R, mutNRAS or both mutations together, 72h after transduction cells were lysed and analyzed by immunoblot for NRAS and hIL7R protein expression.